Correlated measurements of the secondary cosmic ray fluxes at July 17, 2002 by the Aragats Space-Environmental Center monitors

A. Chilingarian, K. Avakyan, V. Babayan, N. Bostanjyan, V. Eganov, A. Hovanissyan, N. Gevorgyan, G. Gharagyozyan, S. Ghazaryan, A. Garyaka, V. Ivanov, H. Martirosyan, R. Martirosov, L. Melkumyan, H. Sogoyan, S. Sokhoyan, S. Tserunyan, A.Vardanyan and M.Zazyan

Cosmic Ray Division, Yerevan Physics Institute, 2 Alikhanyan Brothers, Yerevan, Armenia

Abstract. We demonstrated the sensitivity of the correlation of different species of secondary cosmic ray flux to geophysical conditions. The count rate changes of cosmic ray monitors of the Aragats Space-Environmental Center at July 17 distinguish three distinct phases of the Space Weather events, connected with Solar activity. The correlation analysis could be useful for the understanding of the yet unclear mechanisms of the particle acceleration at Sun and in the interplanetary space.

1. Introduction: July 15-17, 2002 Solar-Terrestrial Connections

At July 16-17, 2002 the cosmic ray flux incident on the Earth and, therefore, secondary fluxes reaching mountain altitudes were highly variable due to C6.5 flare started 6.37 UT July 16 and M8.5 flare started at 6.58 July 17 (accompanied by the Coronal Mass Ejection - CME) and arrival of the shock wave from CME associated with X3.0/3b flare (flare itself wasn't accompanied by the enhancement of the proton flux (see Figure 1) started at 19.59 July 15 and reaching 1AU at 16.04 July 17.

C6.5 flare from July 16 could be associated with enhancement of the ion flux in the interplanetary space detected by ACE and GOES satellites lasting more than 2 days, see Figures 1 and 2.

Aragats Space-Environmental Center (ASEC) monitors detect Ground Level Enhancement (GLE) at July 16 and 17 (see Figures 2 and 3). Some characteristics of the GLE registered by the Neutron Monitors at longitudes from 20^{o}E (Lomnicky Stit) till 101^{o}E (Irkutsk) are posted in Table 1. High latitude monitors register less pronounced enhancements, comparable with low latitude NM. Usually during major proton events due to latitude dependent rigidity the GLEs are much more pronounced at high latitudes.

Particle acceleration to high energies, causing secondary fluxes detectable at high altitudes could be performed

1. during the flare by some not till now fully explained mechanism (Klein et.al., 1999),
2. at a CME shock front in middle and high corona (Reames, 1999) and
3. by acceleration in interplanetary space of the initial seed population ejected by flare (see point 1) by the

some already present in the interplanetary space shock;

4. more exotic acceleration mechanism in “magnetic bottle” structures formed by several shock waves simultaneously present in the interplanetary space also could be considered.

Without going into discussion about validity and preference of the each mechanism (in our previous work, Martirosian et.al., 2002, we demonstrated that first two mechanisms could produce GLE’s), we want only to mention that there were at list 3 shock waves moving in interplanetary space during time of detected GLE. The first was already mentioned CME, caused by July 15 flare. The second was driven by very fast (1100 km/sec) CME launched at 16.00 July 16. And third shock was unleashed by the July 17 M8.5 flare.

The shock wave from July 15 event passed L1 point at 15.29 (one can see in Figure 2 corresponding maximums in He and O ion fluxes registered by the SIS instrument on board of ACE) and generates at 16.04 geomagnetic sudden impulse at 1 AU and Forfush decrease (Fd) registered by the world-wide network of Neutron Monitors at approximately same time.

Therefore we can broadly divide ASEC monitors measurements from 17 July at least to 3 distinct periods:

1. 0 – 7 UT, flux minimally disturbed by the Solar activity;
2. 7 - 14 UT, GLE;
3. 16 - 22 UT, decreasing phase of Fd.

2. ASEC Monitors Count Rates

There are 4 major causes of the changes of ground level monitors count rates connected with solar activity:

1. Additional (to highly constant and isotropy flux of the galactic cosmic rays) solar ions interacting with Earth’s atmosphere nucleus and originated secondary fluxes of the electrons, muons and neutrons and hadrons reaching the mountain altitude and enhancing count rates of the appropriate monitors ;
2. Approaching magnetize cloud is screening the Earth from galactic cosmic rays. This effect is maximal when cloud reaches 1 AU.
3. Same cloud, dependent on the geometry and intersection with magnetosphere is redirected some of galactic cosmic rays, causing anisotropic enhancement in several directions, so called “precursors to Fd” (Munakata et.al., 2000);
4. Rigidity cutoff depression (abrupt changes in the magnitospheric filtration due to south pointed Interplanetary Magnetic Field - IMF) (Kudela and Storini, 2001).

The count rates of the ASEC cosmic ray monitors at July 17 are correlated with three phases of the Space Weather (SW) conditions, as one can see from Figure 3 where left vertical line notifies the start of the GLE and the second – of Fd. Now at Aragats are operating 5 solar monitors:

- Two 18NM64, one located at 2000 Nor-Amberd Neutron Monitor (NANM), second at 3200 m Aragats Neutron Monitor (ANM);
- Solar Neutron Telescope SNT1 (Matsubara et.al., 1999);
- Aragats muon monitor (AMM) with energy threshold 5 GeV and surface 60 m^2 (one minute counts sensitivity is approximately 0.2%);
- Electron & low energy muon monitor (EMM) with energy threshold 10 MeV and surface 15 m^2.

Aragats and Nor-Amberd Multidirectional Muon Monitors are under construction now.

SNT1 detector is a part of world-wide network intended to measure very rare events: neutron fluxes from the Sun, enough strong to reach mountain altitudes. SNT1 consists from $4m^2$x0.6m thick plastic scintillators overviewed by the photomultipliers. Near vertical charged flux ($0 – 30^o$) is vetoed by the anticoincidence shielding formed from 5 cm plastic scintillators. The discriminate analysis of photomultiplier pulse height chooses 4 types of events approximately corresponding to the energy releases of 50, 100, 150 and 200 MeV.

Vetoing system of SNT1 is rejected only 35% of total count rate (Tsuchiya et.al., 2001) (compare with 65% rejection for the Gornergrat neutron detector, fully covered by the vetoing proportional chambers). Therefore at least 30% of the SNT1 count rate for the first 2 thresholds (total rate per m^2 per minute is correspondingly 14000 and 3200) constitutes near horizontal muons and electrons giving energy release up to 100 MeV. Total energy release of electrons and muons traversing horizontally one meter long detector (SNT1 is constructed from four scintillators with separate photomultipliers each having 1 m^2 surface) is approximately 200 MeV. We estimate the light collecting efficiency in the stack of scintillators 1 m long about 50%, therefore we come to maximal expected energy release of muons and high energy electrons ~100 MeV.

Two highest thresholds of the SNT1 (total rate per minute per m^2 is correspondingly 900 and 340), therefore, are selecting neutrons with energies more than 200 MeV (the simulations of detector response and calibration experiments are underway and will be applied for our new neutron detector SNT2, to be installed in the end of year).

Detection efficiency of SNT1 is slowly rising function of the neutron energy and it reaches 30% for energies greater than 200 MeV (this estimate is based only on the simulations and didn't account on limited light collected efficiency of detector). Count rates corresponding to the highest thresholds of SNT1 couldn't be directly compared with count rate of the ANM – ~3500 counts/m^2 /minute, due to the very low threshold of the NM. Detection efficiency of NM started from ~3% at 10 MeV is approaching ~20% at 100 MeV (Shibata et.al, 2001). NANM located 1200 m. (100 g/cm^2) deeper in the atmosphere counts ~1500 neutrons per m^2 per minute.

Muon detector located in the underground hall of experiment ANI (Danilova et.al., 1996), register muons with energies larger than 5 GeV. Low energy muons and electrons are filtering by the 7 m. concrete and 7 m. soil above the detector. Measures of the count rate of the muon detector ~3500 counts/m^2 /minute are rather stable due to good statistical provision and constant temperature at detector location. The low energy electron & muon monitor counting ~30,000 particles per m^2 per minute is utilizing the GAMMA Extensive Air Shower surface array density detectors (Eganov et.al. 2000) and its count rate is influenced by the day-night temperature differences.

3. Correlation analysis of the ASEC monitors data

The correlations were calculated for the all monitors and for all 4 threshold values of SNT1 and for 3 distinct time periods mentioned in the Introduction.

From the Table 2 one can see that there are significant correlations between counts corresponding to the first 2 and last 2 thresholds of SNT1, those proving that first threshold are selected mostly muons, and last 2 - neutrons. The second threshold is selecting both muons and neutrons; therefore it correlated both with first and third thresholds.

These correlations arise because different thresholds are selecting one and the same particles incident the detector volume. There are no correlations between counts of different ASEC monitors in the time period 0 – 7 UT, when the strength of the solar-terrestrial connections was minimal.
For the next time period of 7 – 14 UT correlation matrix (Table 3) demonstrates several nontrivial features.

Aragats muon monitor demonstrates correlations with Neutron monitors. And value of the correlation coefficient is greater for the Nor Amberd comparing with Aragats NM.
This contradiction could be explained if we remember that energy threshold of AMM is 5 GeV and corresponding primary ions have energy approximately ~50 Gev. Therefore, the cascades originated from particles with higher energies will contain neutrons of higher energies comparing with abundant low energy (>7.6 GeV) protons which can penetrate atmosphere at Aragats geographic co-ordinates and generate secondaries reaching mountain altitudes. The correlation with NAMM is greater because higher energy primaries generate secondary neutrons with higher energies which can penetrate till 2000 m.

For the Fd time period correlations are much more pronounced comparing the GLE time span, see Table 4. It is worth to repeat that for the Fd we exactly know that deficit of low energy protons is the main cause of the count rate decrease of secondary CR flux and monitors with low threshold are more sensitive to the Fd than monitors with higher threshold. For example count rate and variance of the AMM didn't change significantly in analyzed time periods, it is equal correspondingly to: 2907±4; 2903±5; 2904±5. In contrast the mean count rate and variance of the monitors having lowest threshold are changing dramatically, the analogical numbers for the count rates corresponding to 1 threshold of SNT1 are: 13964±30; 14053±40; 13757±126.

Differences in the correlations for GLE and Fd time periods could be enumerated by calculating of the so-called Fisher criterion, estimating difference of the pair wise correlations for the same pairs of variables belonging to different classes (in our case different time intervals). From the Table 5 we can see very big values of the Fisher coefficient (values greater than 3 gives only 0.01% probability for the difference to be statistical fluctuation only). Most striking is difference in correlation SNT_1 vs. NANM. If for GLE period this correlation is near zero, for the Fd it reaches very big value of 0.82, corresponding value of Fisher criterion is 23.8!

These drastic differences may be caused by the different type of particles giving rise to GLE and Fd. As we already discuss the deficit of low energy protons is responsible for Fd, on the other hand as we can see from the Figure 2, the abundance of the He and O ions are most probable trigger of the GLE.

4.Conclusion

Precise simulation of the ASEC detectors response to the primary flux with different ion abundances is necessary for drawing particular inference on the type of the event giving detected mo dification of the secondary fluxes.

Nonetheless, the sensitivity of the correlation analysis to the different types of events is clearly demonstrated. The correlation between different species of the secondaries could be useful for the understanding of the yet unclear mechanisms of the particle acceleration at Sun and in the interplanetary space.

Acknowledgements. Work was supported by the ISTC A216 grant. We express gratitude to all groups and organizations posted data in Internet. The possibility to analyze data from satellite detectors and world-wide networks of NM brings new quality to physical inference on Solar-Terrestrial connections and Space Weather.

References

Martirosyan H., et.al., The correlations between GLE fine structure and primary ion type, to be published in *Advances of Space Research*.

Danilova T. V., et al., The ANI experiment on the investigation of the interactions of hadrons and nuclei in energy range 1000 - 100000 TeV, *NIM*, **A323**, 104-107, 1992.

Klein K.-L., et al, Flare-associated energetic particles in the corona and at 1 AU, *A&A*, **348,** 271-285, 1999.

Eganov V., Garyaka A., EAS electron and muon distributions and size spectra from the GAMMA installation, *J.Phys.G: Nucl.Part.Phys.* **26,** 1355, 2000.

Kudela K., Storini M., Direct and Indirect Relations of Cosmic Rays to Space Weather, *Proc. "SOLPA, Vico Equense,* Italy, 289, 2001.

Matsubara, Y., and Muraki, Y., et al., "Observation of Solar Neutrons by the World-Wide Network of Solar Neutron Detectors", *Proc.of 26th ICRC,* **6,** 42, Salt-Lake-City, 1999.

Munakata K., Bieber J.W. et al, Precursors of Geomagnetic Storms Observed by Muon Detector Network, *Bartol Research Institute Preprint,* BA-00-11, 2000.

Reames D.V., Particle Acceleration at the Sun and in the Heliosphere, *Space Sci. Rev.*, **90,** 413, 1999.

Shibata S., Munakata Y., et.al, Detection Efficiency of a Neutron Monitor Calibrated by an Accelerator Neutron Beam, *NIM,* **A463,** 316, 2001 .

Tsuchiya H., Matsubara Y., et al., Detection Efficiency of a new type of Solar Neutron Detector calibrated by an accelerator Neutron Beam, *NIM,* **A463,** 183, 2001.

K. Avakyan, V. Babayan, N. Bostanjyan, A. Chilingarian, V. Eganov, A. Hovanissyan, N. Gevorgyan, G. Gharagyozyan, S. Ghazaryan, A. Garyaka, V. Ivanov, H. Martirosyan, R. Martirosov, L. Melkumyan, H. Sogoyan, S. Sokhoyan, S. Tserunyan, A.Vardanyan, and M.Zazyan, Cosmic Ray Division, Yerevan Physics Institute, Yerevan-36, Armenia

(e-mail: karen@crdlx5.yerphi.am, babayan@jerewan1.yerphi.am, bostan, chili, eganov, armen, nerses, gagik, ssk, alegar, ivanov, or hmart@crdlx5.yerphi.am, martir@lx2.yerphi.am laura, harut, serg, sargis, or aro@crdlx5.yerphi.am, mary@jerewan1.yerphi.am)

Paper number 2002GL016348.
0094-8276/01/2002GL016348$05.00

Paper number 2001GL012345.

Paper numb er 2002GL016348.

Table 1. 17 July GLE registered by low latitude Neutron Monitors

NM	R_c (Gv)	Altitude (m)	Latitude	GLE Maximum (in MSD units)	Start of GLE
ANM	7,6	3200	40,5	4.7	7:25
NANM	7,6	2000	40,5	5.8	7:20
Lomnicky Stit	3,98	2634	49,2	5.9	7:45
Irkutsk	3,64	2000	51,37	3.6	7:25

Table 2. Correlation Matrix for 0-7 hours

	$SNT1_1$	$SNT1_2$	$SNT1_3$	$SNT1_4$	NANM	ANM	AMM	EMM
$SNT1_1$	*	0.51	0.08	0.11	0.22	0.01	-0.07	0.14
$SNT1_2$	0.51	*	0.32	0.28	0.06	0.02	-0.10	0.07
$SNT1_3$	0.08	0.32	*	0.61	-0.001	-0.07	-0.1	-0.03
$SNT1_4$	0.11	0.28	0.61	*	-0.14	-0.08	-0.06	-0.07
NANM	0.22	0.06	-0.001	-0.14	*	0.07	0.04	0.01
ANM	0.01	0.02	-0.07	-0.08	0.07	*	-0.1	-0.07
AMM	-0.07	-0.10	-0.1	-0.06	0.04	-0.1	*	-0.08
EMM	0.14	0.07	-0.03	-0.07	0.01	-0.07	-0.08	*

Table 3. Correlation Matrix for 7-14 hours

	$SNT1_1$	$SNT1_2$	$SNT1_3$	$SNT1_4$	NANM	ANM	AMM	EMM
$SNT1_1$	*	0.55	0.28	0.25	-0.04	0.24	0.14	0.18
$SNT1_2$	0.55	*	0.46	0.28	-0.10	0.10	-0.10	-0.01
$SNT1_3$	0.28	0.46	*	0.72	-0.08	0.06	0.02	-0.01
$SNT1_4$	0.25	0.28	0.72	*	-0.01	0.17	0.15	-0.04
NANM	-0.04	-0.10	-0.08	-0.01	*	0.18	0.38	-0.10
ANM	0.24	0.10	0.06	0.17	0.18	*	0.27	-0.08

AMM	0.14	-0.10	0.02	0.15	0.38	0.27	*	-0.01
EMM	0.18	-0.01	-0.01	-0.04	-0.10	-0.08	-0.01	*

Table 4. Correlation Matrix for 16-22 hours

	$SNT1_1$	$SNT1_2$	$SNT1_3$	$SNT1_4$	NANM	ANM	AMM	AME
$SNT1_1$	*	0.88	0.67	0.50	0.82	0.72	0.54	0.28
$SNT1_2$	0.88	*	0.77	0.55	0.66	0.62	0.45	0.29
$SNT1_3$	0.67	0.77	*	0.76	0.51	0.52	0.35	0.13
$SNT1_4$	0.50	0.55	0.76	*	0.47	0.46	0.31	0.17
NANM	0.82	0.66	0.51	0.47	*	0.46	0.41	0.11
ANM	0.72	0.62	0.52	0.46	0.46	*	0.37	0.16
AMM	0.54	0.45	0.35	0.31	0.41	0.37	*	0.34
AME	0.28	0.29	0.13	0.17	0.11	0.16	0.34	*

Table 5. The Fischer criteria matrix for measuring significance of difference in correlations between 7-14 and 16-22 hours

	$SNT1_1$	$SNT1_2$	$SNT1_3$	$SNT1_4$	NANM	ANM	AMM	EMM
$SNT1_1$	*	15.1	10.3	6.0	23.9	13.0	9.2	2.0
$SNT1_2$	15.1	*	10.5	6.6	17.7	12.6	11.5	6.0
$SNT1_3$	10.3	10.5	*	1.4	12.6	10.2	6.8	2.8
$SNT1_4$	6.0	6.6	1.4	*	10.2	6.5	3.3	4.0
NANM	23.9	17.7	12.6	10.2	*	6.2	0.7	4.2
ANM	13.0	12.6	10.2	6.5	6.2	*	2.3	4.8
AMM	9.2	11.5	6.8	3.3	0.7	2.3	*	7.2
EMM	2.0	6.0	2.8	4.0	4.2	4.8	7.2	*

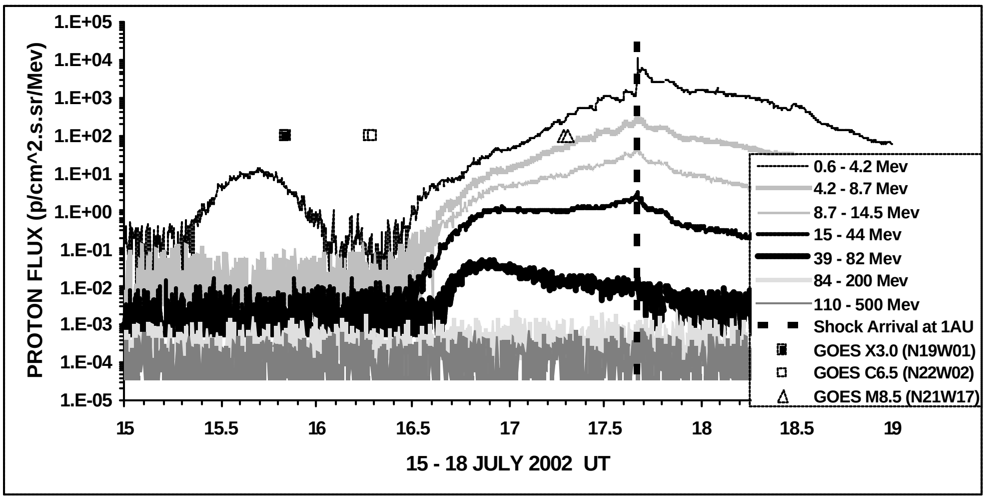

Figure 1. The proton flux variations at 15-17 July 2002
Figure 1. The proton flux variations at 15-17 July 2002

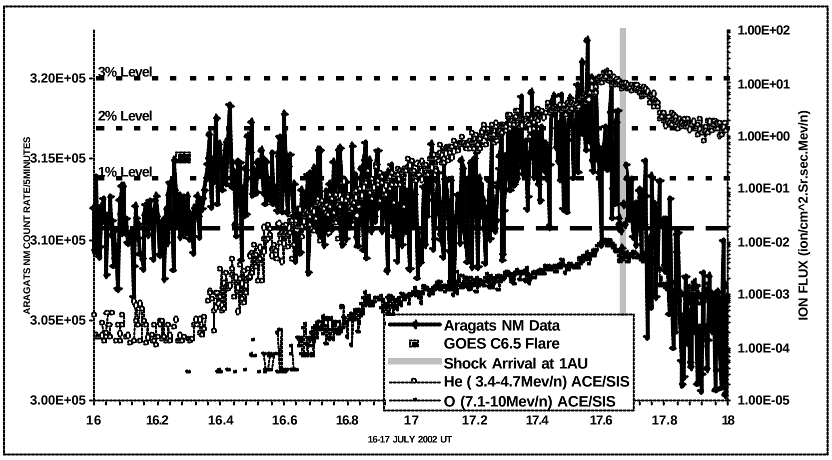

Figure 2. He and O ions flux at 16-18 July 2002, superimposed on the Aragats NM data.

Figure 2 . He and O ions flux at 16-18 July 2002, superimposed on the Aragats NM data.

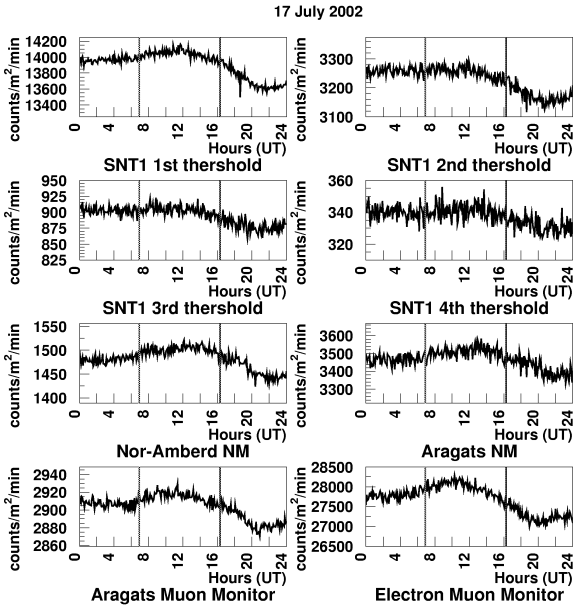

Figure 3. Count rates of ASEC monitors, left line is start of GLE, right line – start of Fd.

Figure 3. Count rates of ASEC monitors, left line is start of GLE, right line – start of Fd.